URN (Paper): urn:nbn:de:gbv:ilm1-2011iwk-125:1

56TH INTERNATIONAL SCIENTIFIC COLLOQUIUM
Ilmenau University of Technology, 12 – 16 September 2011
URN: urn:nbn:gbv:ilm1-2011iwk:5

DYNAMIC WEIGHING CALIBRATION METHOD FOR LIQUID FLOWMETERS -A NEW APPROACH

Jesús Aguilera

PTB Physikalisch-Technische Bundesanstalt, Department of liquid flow
Bundesallee 100 Braunschweig, Germany, D-38116
Tel: +49-531-592-1356, Fax: +49-531-592-1389
E-mail: jesus.aguilera@ptb.de

ABSTRACT

In the last years, the PTB liquid flow group has been working on the development of a new method to calibrate liquid flowmeters under dynamics conditions [1,2]. Such a measurement principle is based on a dynamic weighing approach, which is able to reproduce the unit of mass flow several times, with the ultimate goal to reduce the calibration time, energy cost, and workload in liquid flow calibration laboratories. The calibration method relies on a thorough analysis of the interaction between the acting flow-induced forces present in the measurement process, and the dynamics of the weighing system. The effectiveness of this new calibration method is validated by numerical and experimental tests, in which the obtained results demonstrate that an accuracy level of less than 0,1% is attainable.

Keywords: Liquid flow, primary standard, dynamic weighing, flowmeter calibration

1. INTRODUCTION

As a matter of introduction, it is appropriate to explain the aim of a liquid flow primary standard, how it works, and the difference between a static weighing, and a dynamic weighing liquid flow calibration system.

1.1. Liquid flow primary standard

Firstly, the aim of a liquid flow primary standard is to calibrate the flowmeters from different industrial sectors, wherein the accuracy of this measurand plays a key role in the process output and in the economy. Some of the sectors involved are: oil, chemical, water transport, and the pharmaceutical industry. A liquid flow primary standard is a system designed to have the lowest practical measurement uncertainty, so that this high accuracy can be passed to the flowmeter being calibrated, and subsequently to the process measurement. A unique characteristic of flow primary standards is that, unlike flowmeters, these are capable to reproduce the flow unit by themselves, without reference to some other measuring system of the same quantity (but only to the fundamental units of mass, time, and temperature) [3].

1.2. Static weighing liquid flow primary standard

In terms of its conceptual design, the liquid flow primary standard can be depicted as a hydraulic circuit, in which the liquid is driven by a pumping system, and together with a control valve, set up the operational mass flow rate and fluid pressure (**Fig. 1**). Then, the pumped liquid circulates through a pipeline of different diameter sizes, with the goal to transfer the fluid mass from the Meter Under Calibration (MUC) to a mass reference standard. The MUC section shown in **Fig. 1** is a straight pipeline, which holds the MUC, and it is long enough to allow the flow profile to be swirl-free [4].

Once the process quantities of flow, pressure, and fluid temperature attain a satisfactory level of stabilization, then the calibration test can be initialized. In this instance, the measurement starts when the bypass valve (**Fig. 1**) diverts the fluid flow into a collection vessel supported by a weighing system (mass reference standard), and at the same moment the time counting is initialized (**Fig. 1** and **Fig. 2a**). During the second stage of the measurement run (**Fig. 2b**), the water mass is continuously poured into the collection vessel, and the time counting carries on. Then, after the collection of water mass reaches the prescribed level, the bypass valve re-directs the fluid back to the supply tank and the time counting is stopped (**Fig. 2c**). At this stage of the process, the water mass as well as the weighing system requires some time, in order to attain an equilibrium condition, and once this is achieved, the water mass can be quantified. The outcome from this measurement process is an average mass flow rate $\overline{\dot{m}}_w$ resulting from the totalized water mass m_{Total} in the collection vessel, and the time t_{Total} taken to collect such an amount of fluid (**Eq. 1**).

$$\bar{\dot{m}}_w = \frac{m_{Total}}{t_{Total}} \qquad (1)$$

The principle described above corresponds to the measurement principle of a static weighing liquid flow primary standard, mostly used in flow calibration laboratories. Note that the subindex *w* in **Eq. 1** stands for water as the fluid in use.

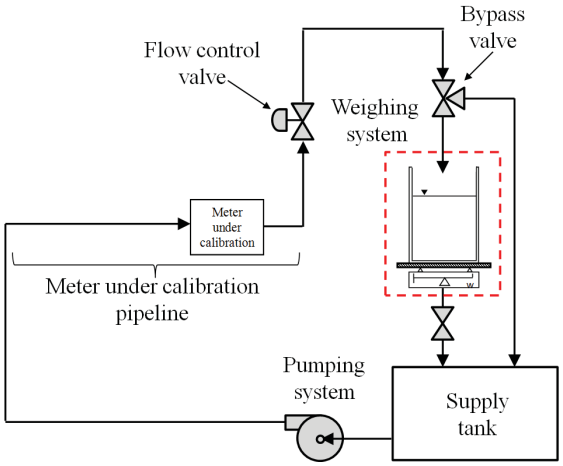

Fig. 1 Schematic diagram depicting the main components of a liquid flow primary standard

1.3. Dynamic weighing liquid flow primary standard

Now, it is necessary to know the difference existing between the recalled static weighing method, and the proposed dynamic weighing approach for the calibration of flowmeters. In order to understand these two different concepts, it is worth analyzing them from the perspective of the mass-time and the mass flow rate- time graphs shown in **Fig. 2.** Firstly, for a dynamic weighing liquid flow measurement, the steps **(a)** and **(c)** shown in **Fig. 2** are disregarded from the process, since this measuring technique is not intended to calculate an average mass flow rate value (from a totalized mass and time), but to estimate the measurand several times during the water mass collection **(b)**.

In order to determine the time-varying mass flow rate by using a dynamic weighing approach, it is necessary to take into account additional physical variables, which are either not present or treated in a different form by a static weighing liquid flow primary standard. These types of variables are the flow-induced forces, such as the acting time-varying fluid force of water jet impact when the fluid is being poured into the vessel. Another force is related with the dynamic oscillatory response of the weighing system, due to the continuous increment of mass, and the elastic properties of its sensing element. A third force involved into the process is the collected water mass force, or the product of the current water mass inside the vessel and the local acceleration of gravity. The upward buoyancy force acting upon the water mass plays also a role, either in a static or a dynamic weighing liquid flow standard.

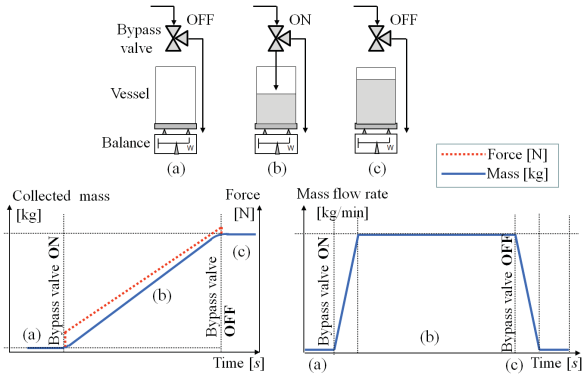

Fig. 2 Measurement principle of a liquid flow primary standard

The situation in a dynamic weighing liquid flow primary standard is that when the weighing system is measuring, it does not longer quantify the collected water mass, but a summation of all the recalled forces, as shown in **Fig. 2**. Therefore, in order to implement this dynamic weighing approach, it is required to identify, and to estimate the magnitude of each of these flow-induced forces. In this instance, the water jet impact force, and the dynamic weighing reacting oscillatory force are classified as unwanted variables, due to the fact that their magnitudes only exist as long as the fluid is in motion. The buoyancy force is also an unwanted variable, which causes the weighing system to measure an apparent loss of mass; however it is a function of the collected water mass. Finally, the collected water mass force is in this case the remaining variable, and also the desired quantity of the process, because its magnitude represents the current mass of water in the vessel under the influence of the local acceleration of gravity (9,8125 m/s²).

When the current collected water mass is quantified, then it is possible to estimate the time-varying mass flow rate $\hat{\dot{m}}_w(t_n)$ as the quotient between the estimate water mass $\hat{m}_w(t_n)$, and its corresponding time t_n during the filling process (**Eq. 2**).

$$\hat{\dot{m}}_w(t_n) = \frac{\hat{m}_w(t_n) - \hat{m}_w(t_1)}{t_n - t_1} \qquad (2)$$

Note that the term *estimate time-varying mass flow rate* (denoted as ^) is given because in practice the flow is in turbulent regime, the pumping system of a primary standard cannot keep at all times an absolute constant flow, the pipe fittings distort the flow profile, and so on [5]. Moreover, the *estimate* term is attributed to the fact, that the mass flow calculation is

based on analytical and experimental approximations of the undesired mechanical-fluid forces, whereby part of their magnitudes will unavoidably remain present in the measurand.

2. DESCRIPTION OF THE MEASUREMENT PROCESS

As a starting point, it must be stated that the input signal of the measurement process is a fluid force quantity. However, in order to make present the force quantity in this dynamic process, it is necessary to produce fluid motion. Therefore, the true mass flow rate $\dot{m}_w(t)$ is in this instance the command input of the system, and also the desired output of the measurement process to be estimated ($\hat{\dot{m}}_w(t_n)$). Note that the subindex *n* denotes the discrete-time form representation of the measurand for its analysis.

Fig. 3 describes in a block diagram, the dynamic weighing liquid flow primary standard, wherein its working principle is explained by three series-connected subsystems: Input, weighing system, and process model. The first subsystem has as an input signal the true mass flow rate $\dot{m}_w(t)$, or command input. This subsystem is responsible for defining the magnitude of all fluid forces involved in the measurement process (input elements), and sum them up, in order to yield an output signal known as total fluid force $F_T(t)$ (reference input), which will interact with the next subsystem, the weighing system.

The second subsystem deals with the mechanical dynamic response of the balance, due to the acting total fluid force $F_T(t)$, in addition to the process noise force $F_q(t)$, caused by the internal vortex flow [6] and the water surface waves in the collection vessel. In the current analysis, the effect of $F_q(t)$ upon the system is not yet treated, however it is depicted in **Fig. 3** as a reminder that is present in the process, and it must be analyzed in future. Note in **Fig. 3** that such a subsystem is divided into three internal blocks, which represent the mechanical components of the balance, its internal low pass filter (LPF), and the continuous/discrete time conversion of the dynamic weighing system output signal, as it is delivered in the real process.

The third subsystem known as process model is an algorithm responsible for estimating the time-varying mass flow rate. In this instance, the calculation procedure of $\hat{\dot{m}}_w(t_n)$ takes as an input the discrete-time balance force response $F_{Bal}(t_n)$, which is used by the hydrodynamic force correction to identify, and to significantly reduce the magnitude of the unwanted flow-induced forces from the process analysis. The output from this inverse method approach [7] is an estimate time-varying mass flow rate $\hat{\dot{m}}_{HF}(t_n)$, with a minimized influence of the flow-induced force, but still accompanied by measurement noise. The second data processing block known as measurement noise filter is in charge of attenuating the unwanted noise greatly (but not exclusively) attributed to the reacting oscillatory force of the dynamic weighing system response. The final outcome of the whole measurement process is then the estimate mass flow rate $\hat{\dot{m}}_w(t_n)$.

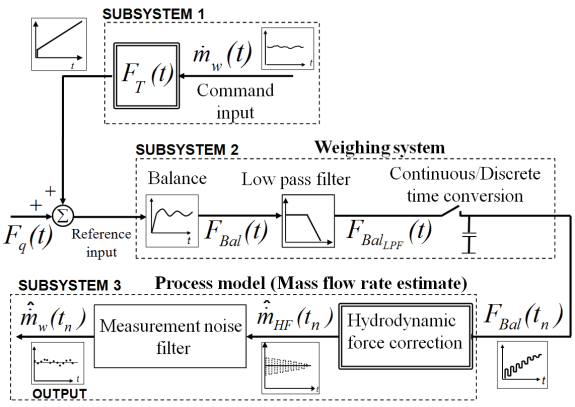

Fig. 3 General block diagram representation of a dynamic weighing liquid flow primary standard and its three main subsystems

3. INPUT SIGNAL

3.1. Collected water mass force

This process variable stands for the force resulting from the collection of water mass inside the vessel, and the effect of the local acceleration of gravity *g* (**Eq. 3**). This variable trends to behave as a ramp function, because of the quasi-continuous pouring of water mass into the vessel, and for the fact that the mass flow rate $\dot{m}_w(t)$ is intended to be at its most stable condition (quasi-steady flow).

$$F_m(t) = \dot{m}_w(t) \cdot g \cdot t \tag{3}$$

3.2. Hydrodynamic force

The second variable involved in the measurement process is known as hydrodynamic force $F_d(t)$, which is caused by the continuous impact of the falling water jet upon the water surface, or the vessel bottom at the initial stage of the collection. In the measurement process, the hydrodynamic force can be represented in a simplified form as:

$$F_d(t) = \dot{m}_w(t) \cdot u_i(t) \tag{4}$$

where $u_i(t)$ stands for the normal impact velocity of the water jet, and in accordance to Bernoulli´s law, this is equal to:

$$u_i(t) = \sqrt{u_n^2(t) + 2 \cdot g \cdot h_i(t)} \qquad (5)$$

In **Eq. 5**, $u_n(t)$ and $h_i(t)$ are respectively the initial velocity of the falling water jet at the nozzle outlet, and its impact height (**Fig. 4**). As for $u_n(t)$,its magnitude will depend upon the constant crossed section area of the nozzle outlet A_n , the density of the fluid ρ_w , and the mass flow rate $\dot{m}_w(t)$. Hence,

$$u_n(t) = \frac{\dot{m}_w(t)}{\rho_w \cdot A_n} \qquad (6)$$

As for the time-varying water jet impact height $h_i(t)$, this can be expressed as the difference between the initial impact height $h_i(0)$ (constant), and the continuously increasing height of the water surface $h_w(t)$ (**Fig. 4**). Thus,

$$h_i(t) = h_i(0) - \overbrace{\frac{\dot{m}_w(t) \cdot t}{\rho_w \cdot A_v}}^{h_w(t)} \qquad (7)$$

where A_v is the cross section area of the vessel.

Finally, after substituting **Eq. 5**, **Eq. 6**, **Eq. 7**, and into **Eq. 4**, it is found that the hydrodynamic force (**Eq. 8**) is a dependent function of the mass flow rate, the fluid density, the local acceleration of gravity as well as the dimensions and geometry of the nozzle outlet, the collection vessel, and the constant initial water impact height.

$$F_d(t) = \dot{m}_w(t) \cdot \left\{ \left(\frac{\dot{m}_w(t)}{\rho_w \cdot A_n} \right)^2 + 2 \cdot g \cdot \left(h_i(0) - \left[\frac{\dot{m}_w(t) \cdot t}{\rho_w \cdot A_v} \right] \right) \right\}^{1/2} \qquad (8)$$

3.3. Buoyancy force

Unlike the other process variables, the buoyancy force $F_b(t)$ acts in normal upward direction; because its magnitude is related to the floating effect the air has upon the water volume. This can be expressed as:

$$F_b(t) = \left(\frac{\rho_A}{\rho_w} \right) \cdot \dot{m}_w(t) \cdot g \cdot t \qquad (9)$$

Here, ρ_A denotes the air density.

3.4. Total fluid force

Now, **Fig. 4** summarizes in a free-body diagram, the graphical representation of all considered forces and parameters involved in the measurement process (**Eq. 10**).

$$F_T(t) = F_m(t) + F_d(t) - F_b(t) \qquad (10)$$

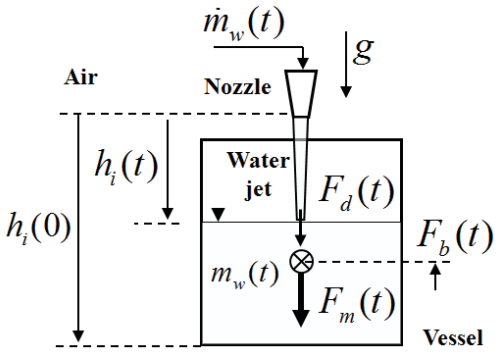

Fig. 4 Free-body diagram of the total fluid force representing the input signal of the dynamic weighing liquid flow primary standard

4. MODELING THE WEIGHING SYSTEM

The main goal of this task is to have a numerical representation of the system, which allows a better understanding of why and how the weighing system responds in a particular way to the given process conditions, such as: the elastic properties of its sensing element, acting fluid forces (intrinsically linked to mass flow rate), the geometry as well as dimensions of its components.

One of the advantages about system modeling is the possibility to quantify the recalled unwanted process variables, and no less important, to identify and to determine the magnitude of some sources of measurement noise. In principle, this identification task can be carried out by experimental means. However, it could turn out to be a quite tedious and complex task without the numerical interpretation of the process, which offers a hint of how to recognize and to separate the process variables. The second significant advantage refers to the concept of verifying the proposed measurement method, not only by experimentally comparing it with the outcome given by a reference flow standard, but also by looking at the results given by the numerical approach.

The proposed numerical model of the weighing system is based on Newton´s third law, and it is restricted to a 1 Degree-of-Freedom (1-DoF), which is the normal axis of weighing (z axis). Such a law states that the acting fluid forces involved in the process (**Eq. 10**), will generate an equal but opposite mechanical force response $\sum F_{Mech}(t)$ exerted by the

weighing system´s cell (represented by a spring and a damping element) and its mass (**Eq. 11**). In other words, **Eq. 11** says that the system struggles at all times for an equilibrium position, due to the continuous alternation of upward and downward forces in the process.

$$F_T(t) = \sum F_{Mech}(t) \tag{11}$$

4.1. Spring force

This is one of the elastic properties of the balance cell that can be represented by a spring element, in which its reacting force denoted by $F_{Bal}(t)$ is equal to the product of the characterized balance stiffness coefficient $k_{Bal}(t)$, and the displacement z undergone by the weighing platform along the collection time (**Eq. 12**).

$$F_{Bal}(t) = k_{Bal}(t) \cdot z \tag{12}$$

4.2. Total mass and inertial force

The second element of the balance is the one dealing with the system's total mass $m_T(t)$, which is equal to the summation of: the collection vessel mass, the weighing platform mass, the possible initial amount of water mass in the collection vessel (all of these represented as m_0), and the increasing time-varying collected water mass $m_w(t)$ depicted in **Fig. 5**.

$$m_T(t) = m_0 + m_w(t) \tag{13}$$

Furthermore, when a dynamic weighing liquid flow measurement is taking place, the continuous alternation of acting fluid forces and reacting mechanical forces causes the system´s total mass $m_T(t)$ to accelerate in an oscillatory form $\ddot{z}$. The result of this dynamic condition is an inertial force $F_{Inertial}(t)$ exerted upon the system, and it is described by **Eq. 14** [8].

$$F_{Inertial}(t) = m_T(t) \cdot \ddot{z} \tag{14}$$

4.3. Damping force

The third element representing the weighing system is related with the inherent characteristic of a balance cell to dampen the oscillatory force amplitude (or to gradually dissipate the energy from the system). In this instance, the damping force $F_c(t)$ can be determined as a product of the system oscillating velocity $\dot{z}$ during the collection process, and the characterized damping coefficient of the weighing system (**Eq. 15**).

$$F_c(t) = c_{Bal}(t) \cdot \dot{z} \tag{15}$$

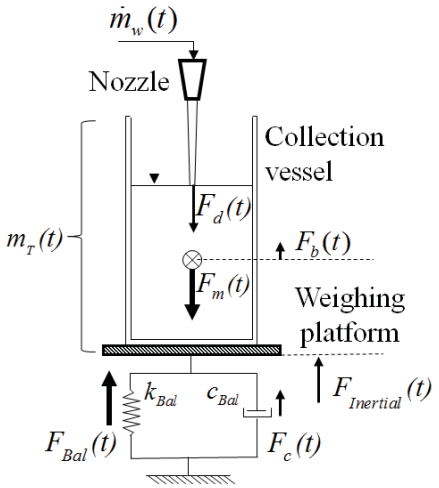

Fig. 5 Free-body diagram describing the analogous representation of the weighing system (elastic and mass elements) as well as the fluid (acting) and mechanical (reacting) forces involved in the process

4.4. 1 Degree-of-Freedom motion equation of the weighing system

Now, at this point, the number of reacting mechanical forces of the weighing system $\sum F_{Mech}(t)$ (**Eq.11**) can be represented as the summation of:

$$\sum F_{Mech}(t) = F_{Intertial}(t) + F_c(t) + F_{Bal}(t) \tag{16}$$

And, on the other hand, the acting fluid forces represented in **Eq. 10** can be also substituted into **Eq. 11**, in order to yield the well known 1 Degree-of-Freedom motion equation applied to the balance:

$$F_m(t) + F_d(t) - F_b(t) = m_T(t) \cdot \ddot{z} + c_{Bal}(t) \cdot \dot{z} + k_{Bal}(t) \cdot z \tag{17}$$

5. THE ESTIMATION OF TIME-VARYING MASS FLOW RATE VIA DYNAMIC WEIGHING (PROCESS MODEL)

5.1. Hydrodynamic force correction

One form to derive an algorithm that can attenuate the presence of the hydrodynamic and buoyancy force from the balance output signal [2], consists in analyzing the 1-Degree-of-Freedom motion equation (**Eq. 17**). In this instance, it is agreed that $F_{Bal}(t)$ describes the balance response, because it is indeed the variable that summarizes in its magnitude the presence of all the recalled acting fluid forces, and on the other hand, it has embedded the reacting balance response. Therefore, it is convenient to express the motion equation as:

$$F_{Bal}(t) = F_m(t) + F_d(t) - F_b(t) - F_{Intertial}(t) - F_c(t) \tag{18}$$

In the real measurement process, the balance is unable to measure each of the fluid force variables independently, but their summation represented by the variable called $F_T(t)$, in addition to the mechanical reacting forces of inertia and damping, Thus,

$$F_{Bal}(t) = F_T(t) - F_{Intertial}(t) - F_c(t) \qquad (19)$$

Now, for the purpose of deriving a practical equation for the determination of mass flow rate, it is necessary to simplify **Eq. 19** based on the physical fact, that the balance force response $F_{Bal}(t)$, and the total acting fluid force $F_T(t)$ are equal in terms of their slope magnitude (**Eq. 20**) [9]. The explanation to this statement is given in the following text below. Note that **Eq. 20** requires to be expressed in a discrete-time form t_n, due to the sampling time of the data acquisition system.

$$F_{Bal}(t) \triangleq F_T(t) \xrightarrow{\text{Discrete time}} F_{Bal}(t_n) \triangleq F_T(t_n) \qquad (20)$$

Firstly, consider the Force-time graph shown in **Fig. 6a**, wherein $F_T(t_n)$ is splitted into its three components: collecting mass force, hydrodynamic force, and buoyancy force. On other hand, take a look to **Fig. 6b**, in which the path of a ramp-like response of $F_T(t_n)$ and $F_{Bal}(t_n)$ are overlapping all along the filling process, and whereby their nominal slope magnitudes are basically the same in both cases. The relatively small difference still remaining between these two state variables $F_T(t_n)$ and $F_{Bal}(t_n)$ is due to the inertial force $F_{Intertial}(t_n)$, the damping force $F_c(t_n)$, in addition to the effect of the system time constant, the continuous-discrete time conversion, and the oscillatory signal attenuation carried out by the internal low pass filter. These remaining signal-conditioned unwanted state variables will be treated by the following data processing algorithm, the measurement noise filter.

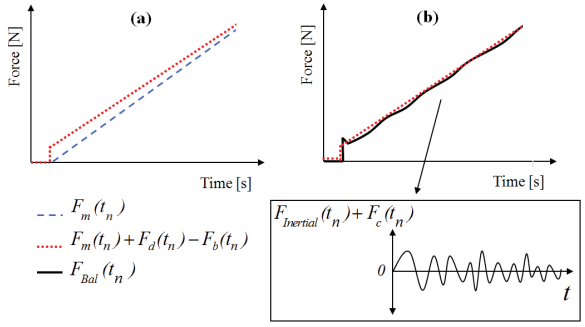

Fig. 6 Graphical representation of (a) acting fluid forces and (b) balance force response during the filling process

In summary, **Eq. 21** gathers the recalled statements in an expression, which says that the balance output response can be equal to the summation of the estimated fluid force variables, denoted by ^.

$$F_{Bal}(t_n) = \hat{F}_m(t_n) + \hat{F}_d(t_n) - \hat{F}_b(t_n) \qquad (21)$$

Then, after re-writing **Eq. 21** as a function of a discrete-time mass flow rate, the equation takes the following form:

$$F_{Bal}(t_n) = \hat{\dot{m}}_{HF}(t_n)\cdot g\cdot t_n + \hat{\dot{m}}_{HF}(t_n)\cdot \hat{u}_i(t_n) - \ldots - \hat{\dot{m}}_{HF}(t_n)\cdot g\cdot\left(\frac{\rho_A}{\rho_w}\right)\cdot t_n \qquad (22)$$

In **Eq. 22**, the subindex *HF* is used instead of *w*, to underline that the mass flow rate estimate will be the outcome of the hydrodynamic force correction. Then, after substituting the hydrodynamic force equation in a discrete-time form (**Eq. 8**) into **Eq. 22**, and applying some algebraic simplifications, it turns out to be that such an algorithm is a polynomial equation of fourth order:

$$\left[\frac{1}{\rho_w^2\cdot A_n^2}\right]\cdot\hat{\dot{m}}_{HF}^4(t_n) - \left[\frac{2\cdot g\cdot t_n}{\rho_w\cdot A_v}\right]\cdot\hat{\dot{m}}_{HF}^3(t_n) + \ldots + \left[2\cdot g\cdot h_i(0) - g^2\cdot\left(1-\frac{\rho_A}{\rho_w}\right)^2\cdot t_n^2\right]\cdot\hat{\dot{m}}_{HF}^2(t_n) + \ldots + \left[2\cdot F_{Bal}(t_n)\cdot g\cdot\left(1-\frac{\rho_A}{\rho_w}\right)\cdot t_n\right]\cdot\hat{\dot{m}}_{HF}(t_n) - F_{Bal}^2(t_n) = 0 \qquad (23)$$

5.2. Measurement noise filter

So far, the hydrodynamic force correction (first algorithm of the process model subsystem) enables to separate, or at least to attenuate some unwanted process variables from the measurand.

Now, the second process model subsystem, known as measurement noise filter is dealing with one particular issue: The system is still unable to calculate in a more precise form the value of the measurand $\dot{m}_w(t_n)$, because it introduces its own system dynamic response into the estimate measurand $\hat{\dot{m}}_{HF}(t_n)$, which adds in a major or a minor degree, *measurement noise* $v(t_n)$. Hence,

$$\hat{\dot{m}}_{HF}(t_n) = \dot{m}_w(t_n) + v(t_n) \qquad (24)$$

An alternative data processing algorithm used in this investigation to treat the embedded measurement noise in the measurand is the *linear Kalman filter* [10]. Such a filter is a computational algorithm that

combines all available measurement data $\hat{\dot{m}}_{HF}(t_n)$ with the knowledge of the system, the statistical description of measurement noise, and the initial conditions of the measurand, in order to estimate the mass flow rate variable $\hat{\dot{m}}_w(t_n)$.

For the aim to determine the magnitude of the estimate measurand from the acquired data $\hat{\dot{m}}_{HF}(t_n)$, it is necessary first, to have a model depicting the general behavior of the mass flow rate, and the measurement noise $v(t_n)$. In this instance, it is possible to agree that the measurand model of the Kalman filter can be equal to the average mass flow rate from the hydrodynamic force correction (**Eq. 25**). The reason for supporting this statement is based on the fact that the measurement process is carried out at the best possible steady flow conditions. Furthermore, from the statistical point of view, the given average or expected value does not imply the true magnitude of the measurand, but the value with a much higher probability of getting closer to it [11]. This is in comparison to the highly spread measurement data.

$$\bar{\hat{\dot{m}}}_{HF} = \frac{1}{N} \cdot \sum_{n=1}^{N} \hat{\dot{m}}_{HF}(t_n) \tag{25}$$

where N is the number of acquired measurement data.

In regards to the measurement noise $v(t_n)$, it can be described as a variable with a N number of data, that approaches to a normal probability distribution $p(v)$, with a zero mean value, and a variance σ_v^2, as shown in **Eq. 26** and **Eq. 27** [11].

$$p(v) \sim N(0, \sigma_v^2) \tag{26}$$

$$\sigma_v^2 = \sqrt{\frac{1}{N-1} \cdot \sum_{n=1}^{N} \left(v_K(t_n) - 0\right)^2} \tag{27}$$

In practical terms, the true measurement noise variance cannot be exactly determined; however it can be fairly estimated by calculating the variance σ_{HF}^2 (**Eq. 28**) of the filter input data $\hat{\dot{m}}_{HF}(t_n)$. The reason for defining it as an experimental estimation of the measurement noise variance and not as an equality (**Eq. 34**) is based on the fact that, σ_v^2 is a direct function of the measurement noise data. On the other hand, σ_{HF}^2 is a function of the measurement data (**Eq. 30**), which does take into account the narrowband distribution of the true measurand values embedded in the spread measurement noise (**Fig. 7**).

$$\sigma_{HF}^2 = \sqrt{\frac{1}{N-1} \cdot \sum_{n=1}^{N} \left(\hat{\dot{m}}_{HF}(t_n) - \bar{\hat{\dot{m}}}_{HF}\right)^2} \tag{28}$$

$$\sigma_v^2 \triangleq \sigma_{HF}^2 \tag{29}$$

In a general basis, the linear Kalman filter estimates the mass flow rate by using the recalled system information, and thus generating a form of feedback response, as shown in **Fig. 7**. This means, the filter estimates the mass flow rate at some time n, then it feedbacks a value $\hat{\dot{m}}_w(t_{n-1})$, which serves as a prediction for the next time step, and compares it with the current measurement value $\hat{\dot{m}}_{HF}(t_n)$, in order to estimate the measurement noise $\hat{v}(t_n)$ still embedded in the estimate values.

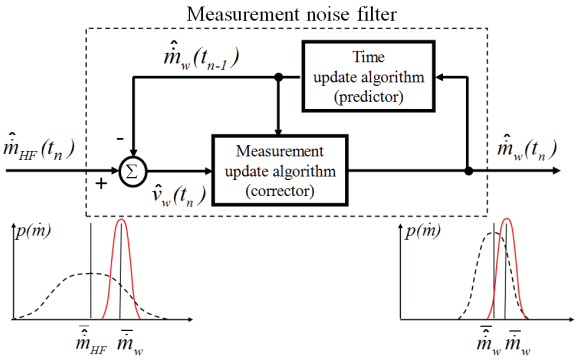

Fig. 7 Basic description of the linear Kalman filter cycle used as a measurement noise filter

As depicted in **Fig. 7**, the operation of the Kalman filter is divided into two linked algorithms called [10]: the *time update (predictor) and the measurement update (corrector) algorithms*. In this instance, the time update algorithm is in charge for projecting forward (in time) the current measurand and its error variance estimate, so an *a priori estimate* can be obtained for the next time step. On the other hand, the measurement update algorithm will be responsible for using the *a priori measurand estimate*, and the current measurement noise estimate, in order to yield a new improved *a posteriori measurement estimate.* As a remark, the given information regarding to the measurement noise filter (Linear Kalman filter) is described here in a general basis, as a statistical tool to estimate the mass flow rate via dynamic weighing. However, if the reader is interested in knowing more in detail the full content of this algorithm, reference [10] is recommended as an introductory explanation.

6. NUMERICAL AND EXPERIMENTAL DETERMINATION OF THE TIME-VARYING MASS FLOW RATE

6.1. Experimental setup

For the experimental tests of the proposed calibration method, a prototype of a dynamic weighing liquid

flow primary standard was built. Such a prototype comprises a source of quasi-steady flow, a control valve to set the desired flow rate, a connecting pipe, a PTB reference flow standard (Turbine flowmeter with a measurement uncertainty of ±0,1% at 95% confidence level), a bypass valve (with non-fast actuation required), and a 10-L collection vessel.

As for the weighing system in use, it is a commercial 30-kg Electromagnetic Force Compensation cell [12], with a resolution of 0,1 g, a maximum data sampling rate of 25 Hz for this particular application, and an internal low pass filter with a cutoff frequency of 10 Hz. The data acquisition system for used for this prototype was able to record the balance output signal at a rate of 250 samples/s with its corresponding time stamp. The operational flow range of the rig is from 3 kg/min to 8 kg/min through a 25-mm diameter pipeline.

6.2. Hydrodynamic force correction

As recalled, the hydrodynamic force correction is implemented with the goal to enhance the measurement accuracy of the mass flow rate estimate. In this instance, the most illustrative way to see the benefit on implementing this correction is when comparing the mass flow rate obtained by such an approach, and by simply using the balance output response to estimate the mass flow rate (**Eq. 30**).

$$\hat{\dot{m}}_{Bal}(t_n) = \frac{F_{Bal}(t_n) - F_{Bal}(t_1)}{g \cdot (t_n - t_1)} \qquad (30)$$

As for the numerical results, the average value of hydrodynamic force correction output signal is able to get really closer to the true measurand. The percent relative error found at 8 kg/min is 0,01%, in comparison to 0,24% when none corrections to the weighing system output signal are made (**Fig. 8**).

Note that the second measurement data yield by the Hydrodynamic force correction (**Fig. 8**) is just as spread as the balance readout approach described in **Eq. 30**. This means, a maximum relative error of ±2,43% with respect to its average value at 5s, and a gradual decrement of up to ±0,25% at 55s.

Concerning to the experimental mass flow rate estimates, the direct balance output signal approach (**Eq. 30**) reveals a relative error of about 0,20 % in relation to the average reference value given by the transfer standard (**Fig. 8**). On the other hand, a smaller relative error of 0,07% is attained when using the hydrodynamic force correction to estimate the flow unit.

As seen in **Fig. 8**, the hydrodynamic force correction has remarkably improved the accuracy of the calculated time-varying mass flow rate, in relation to the balance output signal approach (**Eq. 30**), which overlooks the induced force of the impacting water jet as well as the buoyancy force. Now, the second algorithm of the process model (measurement noise filter) will address the task of improving not only the accuracy but mainly to obtain measurand estimates with a higher precision.

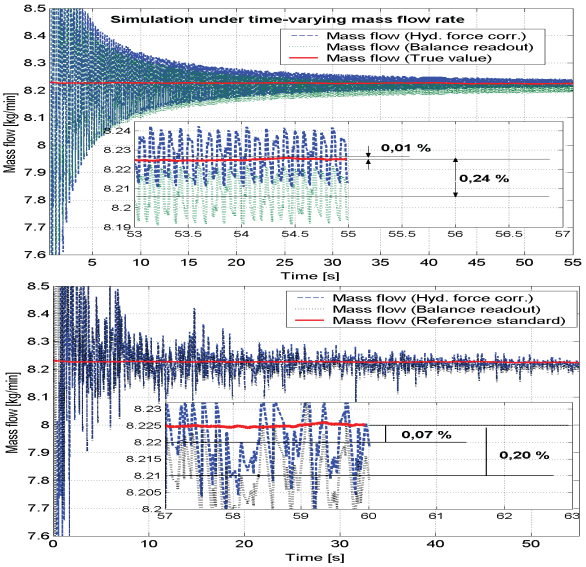

Fig. 8 Numerical (Upper graph) and experimental (Lower graph) response of the hydrodynamic force correction and its effect upon the measurement accuracy

6.3. Measurement noise filter

In this simulation performed at a nominal mass flow rate of 8 kg/min, the measurement noise filter was able to converge relatively fast the true time-varying mass flow rate (**Fig. 9**). Moreover, the largest difference found between both data was 0,1%, and it took place during the first second of the estimation process. A particular characteristic observed in the filter response is that besides following the quasi-steady mass flow rate, its scattered data served as a band that covers the time-varying measurand all along the process. A similar response occurs at 3 kg/min. From this numerical test, the measurement noise filter was able to perform an approximate of 11250 estimates, with an accuracy of ±0,05% after 10s at 8 kg/min.

In relation to the 3 kg/min, the true mass flow rate exhibits a slight decrement in its magnitude, and in response, the filter is able to track the same trend. Furthermore, despite the fact that some estimate values are out of the band, this does not represent a major issue, because the maximum difference found is 0,02% at 50s.

As a remark, the simulation data of the true mass flow rate were directly acquired from the reference flowmeter used during the experimental tests. The reason for doing that is with the aim to have an

approximately equal input, so that the numerical and experimental approaches to be compared. Moreover, this is also a verification tool that serves to evaluate the level of closeness and consistency of the numerical model results with respect to the physical system.

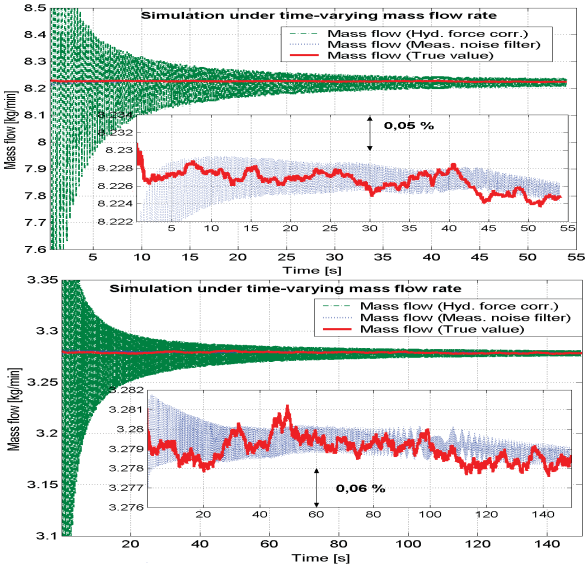

Fig. 9 Numerical results of the measurement noise filter

As for the experimental results at 8 kg/min, the measurement noise filter approaches rapidly to the reference data. The largest difference between both measurement principles was 0,05% at the very beginning of the estimation process (**Fig. 10**). Another interesting feature observed at this flow rate is that the filter is able to follow the fluctuating flow (according to the transfer standard) from time 5s to 20s. In general, the measurement noise filter kept an uniform response with a percent difference of 0,025%.

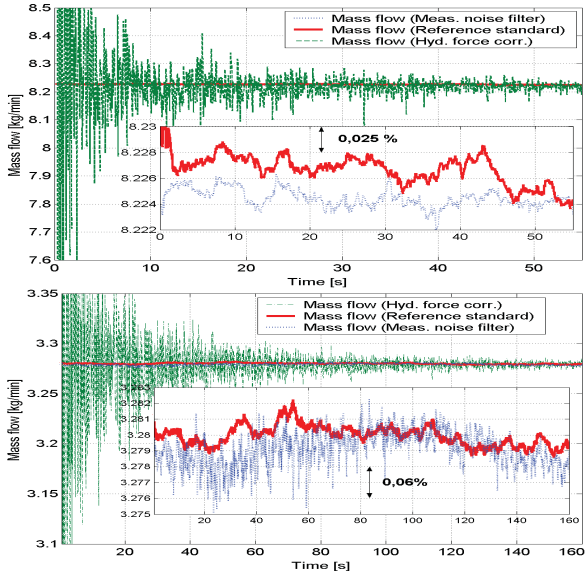

Fig. 10 Experimental results of the measurement noise filter

At 3 kg/min, the measurement noise filter performs its best estimate, because its output practically follows at all times the time-varying mass flow rate reference. Even the data scattering of ±0,03% from the filter is convenient, because it ensures that the estimate values are within the reference. The filter output signal delivers in this case around 37500 estimates (at 3 kg/min).

6.4. The influence of data sampling frequency and the low pass filter cutoff frequency upon the mass flow rate estimate values

When dynamic weighing mass flow measurements are performed experimentally, the outcome is at some degree limited by the balance manufacturer design specifications. In this instance, it is referred to the maximum data sampling frequency that the balance readout can deliver, and the internal filter algorithm (customized low pass filter) used to attenuate the undesired oscillatory response of the balance. The following numerical simulation exemplifies the effects of the data sampling frequency as well as the low pass filter upon the measurand by changing their parameters. The main goal of comparing these results with the obtained so far is to understand how such parameters can significantly impact in the determination of the measurand [13], and what can be done in practice, in order to bring more accurate and precise mass flow rate measurements.

At first, **Fig. 11** exemplifies the filter response when the low pass filter is taken into account at its corresponding setup specifications (cutoff frequency: 10 Hz), and at a data sampling frequency of 30 Hz. In this example, the estimate values exhibit a prompt convergence to the true mass flow rate values, despite the data spread at the beginning of the process. This initial behavior can be associated with the influence of the large measurement noise at the initial stage.

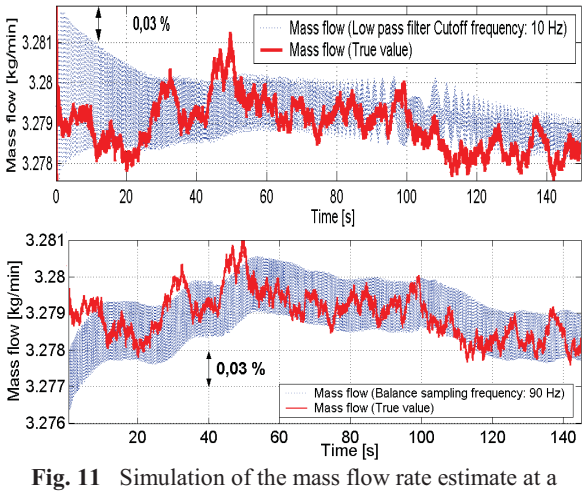

Fig. 11 Simulation of the mass flow rate estimate at a balance data sampling rate of 30 Hz and a low pass filter cutoff frequency of 10 Hz (Upper graph), and at a higher data sampling rate of 90Hz and no low pass filter (Lower graph)

On the other hand, the performance of the filter is remarkably improved when the system is able to sample data at a higher frequency of 90 Hz, and without a low pass filter. In this case, the estimate values converge in a few seconds after the starting point of the collection process. Moreover, it is observed that the filter keeps a better tracking of the fluctuating mass flow rate within ±0,025%, in relation to the average value of the true measurand data.

In summary, after comparing these two cases, it is clear that indeed the accuracy and precision of the estimate values can be re-enhanced if the balance output signal could avoid the low pass filter, and the data sampling frequency was higher. However, the important issue to remark here is that the adequate increment of the data sampling frequency will mainly depend on the level of the stationary fluctuating flow undergone by the primary standard and the balance time constant. Furthermore, as an important remark, these specific output signal characteristics can be realized (at present) only by customized balances.

7. CONCLUSIONS AND REMARKS

After analyzing the proposed method for the calibration of liquid flowmeters, the following conclusion and remarks can be made:

- It is necessary and feasible to simulate the measurement process, with the aim to understand the system dynamic response, what are the main sources of noise in the process and from where they are coming from, the role and significance of different process variables, and to verify the consistency of the experimental results with the proposed theory. In this instance, the simulation applies to a 1 degree-of-Freedom, which despite only analyzing the normal weighing system, it highlights the most striking fluid-mechanical forces in the process: 1) the water jet impact force as well as the collected mass force and the buoyancy force, and 2) the normal reacting force of the weighing system,

- The inverse problem approach applied by the hydrodynamic force correction proves its effectiveness in greatly reducing the unwanted effect of the flow-induced force upon the measurand,

- The linear Kalman filter is an appropriate data processing tool to attenuate the measurement noise from the measurand, and as demonstrated in simulation and experiments, it keeps respectively a good tracking of the quasi-steady mass flow rate,

- According to the carried out tests, accuracy levels smaller than 0,1% by applying the dynamic weighing liquid flow calibration approach are attainable,

- This new measurement approach can significantly shorten the time of a calibration by only requiring a single measuring run (collection) per mass flow rate when characterizing a flowmeter, and also delivering a larger amount of measurement data,

- The accuracy and precision of the estimate measurement can be significantly enhanced if the data sampling frequency of the weighing systems was increased, and the low pass filter was avoided. However, the criteria for an appropriate increment of the data sampling frequency will be closely related with the level of stationary fluctuating flow at the primary standard and the balance time constant. Moreover, as a remark, these specific output signal characteristics can be currently provided only by customized balances.

- In a following research, the process noise $F_q(t)$ caused by the flow-induced force inside the collection vessel has to be investigated, and incorporated into the Kalman filter algorithm, in order to re-enhance the current measurement accuracy and precision.

8. NOMENCLATURE

A_n : Cross section area of the nozzle outlet
A_v : Cross section area of the collection vessel
c_{Bal} : Damping coefficient
$F_b(t)$: Buoyancy force
$F_{Bal}(t)$: Balance force response
$F_c(t)$: Damping force
$F_d(t)$: Hydrodynamic force
$F_{Inertia}(t)$:Inertial force
$F_m(t)$: Collected water mass force
$F_q(t)$: Process noise force
$F_T(t)$: Total fluid force
g: Local acceleration of gravity
$h_i(t)$: Water jet impact height
$h_w(t)$: Water surface level
k_{Bal} : Weighing system stiffness coefficient
$\hat{\dot{m}}_{Bal}(t_n)$:Estimate mass flow rate by balance output response
$\hat{\dot{m}}_{HF}(t_n)$:Estimate mass flow rate by hydrodynamic force correction
$m_T(t)$: Weighing system total mass
m_{Total} : Totalized water mass (static weighing)
$\hat{m}_w(t_n)$: Estimate water mass
$\dot{m}_w(t)$: Mass flow rate
$\hat{\dot{m}}_w(t_n)$: Estimate mass flow rate
m_0 : System mass before collection process
t: Continuous time
t_n : Discrete time
t_{Total} : Total time of collection (static weighing)
$u_i(t)$: Water jet impact velocity
$u_n(t)$: Water jet velocity at the nozzle outlet
$v(t_n)$: Measurement noise
z : Weighing system displacement
$\sum F_{Mech}(t)$:Summation of mechanical forces
ρ_A : Air density
ρ_w : Water density
σ^2_{HF} : Variance of estimate mass flow rate data by hydrodynamic force correction
σ^2_v : Measurement noise variance

9. REFERENCES

[1] R. Engel, "Dynamic weighing-Improvements in gravimetric liquid flowmeter calibration", 5th International symposium on fluid flow measurement, Arlington, VA, USA, April 8-10, 2002

[2] J. Aguilera, R. Engel, G. Wendt, "Dynamic weighing liquid flow calibration system -Realization of a model-based concept", FLOMEKO 2007, Johannesburg, South Africa, Sept. 18th-21st, 2007

[3] Bureau International des Poids et Mesures, "International vocabulary of metrology (VIM)", BIPM, Cedex, France, 2008

[4] R. Baker, "Flow measurement handbook", Cambridge University press, USA, 2000

[5] A. Sleigh, C. Noakes, "The momentum and Bernoulli equations", Leeds University, UK, 2009

[6] X. Weilin, L. Hausheing, "Turbulent flow and energy dissipation in plunge pool of high arch dam", Journal of hydraulic research, Vol. 40, UK, 2002

[7] L. Brusquet, O. Oksman, "Improving the accuracy of tracer flow-measurement techniques by using an inverse-problem approach", Measurement science and technology journal, Vol: 10, P. 559-563, UK, 1999

[8] D. Findeisen, "System dynamics and mechanical vibrations", Springer-Verlag, Berlin, Germany, 2000

[9] P. Sydenham, "Static and dynamic characteristics of instrumentation", CRC Press, University of Southern Australia, Section 3.2, Australia, 2000

[10] A. Gelb, "Applied optimal estimation", MIT Press, P. 102-119, Cambridge, USA, 1974

[11] J. Taylor, "An introduction to error analysis", 2nd edition, University science books, P.137-141, Sausalito, CA, USA, 1997

[12] A. Reichmuth, "Measuring mass and force with a balance", Mettler Toledo, V.12, Greifensee, Switzerland, June, 1999

[13] P. Ribeiro, "Time-varying waveform distortion in power systems", Chapter 15, 1st Edition, Wiley and Sons, USA, September, 2009